Hindawi
Advances in Materials Science and Engineering
Volume 2019, Article ID 5725708, 10 pages
https://doi.org/10.1155/2019/5725708

Research Article

Stability Analysis of Soil Embankment Slope Reinforced with Polypropylene Fiber under Freeze-Thaw Cycles

Yafeng Gong,[1] **Yulong He**,[1] **Chunpeng Han**,[2] **Yangfan Shen**,[1] **and Guojin Tan**[1]

[1]*Jilin University, College of Transportation, Changchun 130025, China*
[2]*Northeast Forestry University, College of Civil Engineering, Harbin 150040, China*

Correspondence should be addressed to Guojin Tan; tgj@jlu.edu.cn

Received 16 October 2018; Accepted 24 December 2018; Published 21 January 2019

Academic Editor: Ali Nazari

Polypropylene fiber is a common soil reinforcement material which is used to reinforce a common clay in northeast China. Numerical analysis method was performed to investigate the effect of polypropylene fibers on stability of embankment slope subjected to freeze-thaw cycles. The orthogonal experiments of three factors (freeze-thaw cycle, fiber content, and fiber length) and three levels were carried out, and the corresponding nine groups of specimens were made, whose shear strength parameters (internal friction angle and bond force) were measured by direct shear test. Then, the experimental results were analyzed by analysis of variance and range analysis so that the optimum fiber content and fiber length can be determined. The finite element model of typical high-fill soil slope of freeway in northeast China was established whose basic material parameters were taken as the parameters of shear strength of different freeze-thaw cycles under the optimum fiber content and fiber length. The concept of shear strength reduction was introduced into the finite element model, and the convergence of the finite element model was taken as the judging criterion of slope stability. Thus, stability analysis of soil embankment slope reinforced with polypropylene fiber under freeze-thaw cycles was realized. The results show that the addition of fibers improves the cohesion under the action of freeze-thaw cycles, and the internal friction angle is improved in the case of freezing and thawing. This phenomenon leads to the improvement of the stability of the embankment slope in a freeze-thaw cycle. The improvement is particularly noticeable in the case, and this improvement effect decreases as the number of freeze-thaw cycles increases.

1. Introduction

It is ordinary in seasonal frozen regions such as northeast China that the instability of soil slope continues to emerge due to freeze-thaw (F-T) cycles [1]. Slope stability under F-T cycles has been demonstrated by laboratory experiments and numerical simulations in current research studies [2–7]. The main reason of slope instability is that shear strength parameters of soil vary considerably under F-T cycles [8–10]. Therefore, the preliminary study of slope instability in seasonal frozen area is necessary to investigate the shear strength variation of slope soil under F-T cycles.

Generally, the performance of soil under F-T cycles can be effectively improved by reinforcement materials. The F-T behavior of reinforced soil with inorganic binders has been studied, and test results revealed that its F-T behavior presented the favorable improvement. Adding lime to soil is a proven technique for improving the strength and stabilization of soil [11–13]. In addition, there are other scholars who increased the strength of soil under F-T by adding fly ash to soil [14, 15]. However, these chemical additives usually lead to the high stiffness and less suitability for soil.

As a new type of soil reinforcement technology, fiber-reinforced soil technology is widely used in embankment retaining wall, slope, soft soil foundation, and bridge abutment backfill engineering [16–18]. Because of the advantages of good dispersing ability, higher inertia, and uniform enhancement effect, a practical application prospect of fiber-reinforced soil has been attracting more attentions [19–23]. Random addition of dispersed palm fiber to clay can improve its consolidation and shear behavior [19]. Hay of

wheat was added to swelling clay to improve and stabilize its mechanical and deformation properties [20]. The addition of sisal fiber into silty clay improves its strength, deformation, and shear failure characteristics [21]. It was concluded that the shear strength of clay can be significantly improved by random distribution of coir fibers through a series of consolidated undrained triaxial compression tests [22]. Akbulut et al. found that polypropylene fiber added into soil can effectively improve its compressive strength, and the optimum content is 0.2% according to the unconfined compression strength results [23]. A series of studies have shown that fiber can effectively improve the F-T resistance of soil, and the peak stress of unreinforced and reinforced soil usually decreases when F-T cycles increase. Soil samples reinforced with polypropylene fibers usually behave in a more ductile than unreinforced samples [24]. Roustaei et al. showed that soil reinforced with polypropylene fiber can reduce the influence of F-T cycle on cohesive force of soil [25]. Ghazavi and Roustaie found that the unconfined compressive strength of clay samples decreased by 20–25% with increasing F-T cycles. In addition, the unconfined compressive strength of clay can be improved by adding fiber to clay sample. Moreover, it can be concluded that adding 3% polypropylene fibers leads to the increase of unconfined compressive strength of soil before and after applying F-T cycles by 60% to 160% and decrease of frost heave by 70% [26]. The addition of geofiber and synthetic fluid can improve the California bearing ratio (CBR) performance of fine-grained soils under different freezing and thawing conditions [27].

In this study, polypropylene fiber was adopted to strengthen a common clay in northeast China, and the optimum fiber length and content were also obtained by the orthogonal test. A finite element model of typical high-fill soil slope of freeway in northeast China was established, thus the stability analysis of soil embankment slope reinforced with polypropylene fiber under F-T cycles has been realized. The innovations of this paper are mainly reflected in the following aspects: (1) the research thinking is extended from the layer of material mechanical properties to the level of structural stability, which is more in-depth and systematic; (2) the object of numerical analysis is the typical high-fill soil slope, which is very close to the engineering practice so that the research results are easy to be popularized and applied in engineering practice.

2. Materials and Methods

2.1. Materials. The soil material in this study is a typical soil in northeast China, which was from a construction site in Harbin, China. The sampling depth was 1.2–1.5 m, and the sample color was yellow brown. The proportion, liquid plastic limit, and heavy compaction tests of soil samples were carried out to determine the main physical properties of soil samples according to JTG E40-2007 [28]. Corresponding results are listed in Table 1. According to the screening experiment of soil, the particle-size distribution of the soil was obtained, and the particle-size distribution curves of the soil are shown in Figure 1.

Polypropylene fiber is a kind of synthetic fiber obtained by isotactic polypropylene as raw materials which has good tensile strength, excellent manufacturing stable performance, good corrosion resistance, and antiability after some processes. Thus, it is one of the most common engineering reinforcement materials and widely applied to engineering projects. The polypropylene fiber used in this study is white, soft, and smooth textured monofilament fiber-shaped strip (shown in Figure 2), which was obtained from the Hebei Hongxing company. The main physical and mechanical parameters of the polypropylene fiber are given in Table 2.

2.2. Test Scheme. The F-T cycles, fiber content, and fiber length are the three most important factors for the shear strength parameters (internal friction angle and cohesion) of fiber-reinforced soil. Taking these three factors as control factors, the orthogonal experiments of fiber-reinforced soil were designed with three factors and three levels, and nine groups of fiber-reinforced soil were determined, which are listed in Table 3. The previous studies showed that the soil has reached a new balance after 6 F-T cycles, whose physical and mechanical properties changed little [29–31]. Therefore, the maximum F-T cycles in this test was set as 6 cycles. A series of direct shear tests of fiber-reinforced soil were carried out under the optimum water content condition by Welker and Josten, and the optimum fiber content was determined to be 0.2% through the maximum shear strength [32]. Therefore, the fiber content in this paper is taken as 0.1%, 0.2%, and 0.3%. The shear strength parameters of 9 groups of fiber-reinforced soil specimens were tested using direct shear test, and the optimum fiber content and fiber length can be determined by comprehensive analysis.

The optimum fiber content and fiber length were used for fiber-reinforced soil specimens, and the ordinary soil specimen was also made. The shear strength parameters of ordinary soil and fiber-reinforced soil under 0, 1, 3, and 6 F-T cycles were tested, respectively. The reinforcement mechanism of fiber on soil under F-T cycles was analyzed by comparing the variation of shear strength parameters with F-T cycles for fiber-reinforced soil and ordinary soil.

2.3. Test Methods. Based on compaction test, the optimum moisture content of soil can be obtained as 11.4% (Table 1). Water was added to soil based on the optimum moisture content after drying and crushing, and then soil and fiber were mixed thoroughly and evenly following the designed experimental scheme. According to the provisions of the "Technical Specifications for Construction of Highway Subgrade" (JTG F10-2006) [33], the static pressure method was adopted to compact specimens in accordance with the compaction degree of 96%. The low-temperature test device (ADX-300-40) was used for F-T cycles, and the precision of F-T temperature can be controlled within 0.1°C. According to the temperature monitoring data of subgrade in cold regions, the freezing temperature was set as −15°C and the melting temperature was set as 15°C. One F-T cycle lasts for 24 hours (the freezing and melting need 12 hours, respectively).

Table 1: Physical properties of soil samples.

Properties	Specific gravity	Maximum dry density (g/cm^3)	Optimum water content (%)	Liquid limit (%)	Plastic limit (%)	Plasticity index (%)
Value	2.65	1.86	11.4	33.3	24.0	9.3

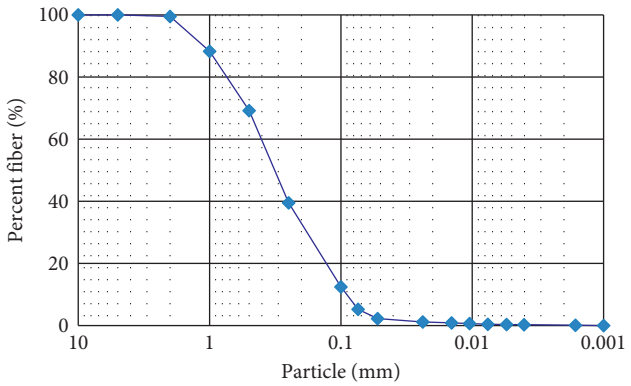

Figure 1: Particle-size distribution curves of soil.

(a) (b)

Figure 2: Materials: (a) polypropylene fiber; (b) fiber soil.

Table 2: Physical and mechanical parameters of polypropylene fiber.

Properties	Density (g/cm^3)	Breaking tensile strength (MPa)	Modulus of elasticity (MPa)	Elongation (%)	Diameter (μm)	Melting point (°C)
Value	0.96	500	3850	10–28	18–48	165

Table 3: Experimental scheme based on orthogonal design.

Specimen number	F-T cycle (time)	Fiber length (mm)	Fiber content (%)
1	1	12	0.3
2	1	6	0.1
3	1	9	0.2
4	3	12	0.1
5	3	9	0.3
6	3	6	0.2
7	6	6	0.3
8	6	9	0.1
9	6	12	0.2

During F-T cycles, specimens were wrapped with multilayers of plastic wrap to prevent water loss.

According to the provisions of the "Test Methods of Soils for Highway Engineering" [28], the SDJ-II type three-speed electric strain direct shear instrument, made by Nanjing Soil Instrument Company, was used for test scheme design of soil samples. The controlling loading rate was 0.8 mm/min for shearing, and the test was completed within 3–5 min. The precision of shear displacement measurement was controlled by 0.01 mm scale indicator. Four specimens were used for each shear group, which were cut to crush under the vertical pressure of 50 kPa, 100 kPa, 200 kPa, and 300 kPa, respectively.

3. Results and Discussion

3.1. Determination of Optimum Fiber Content and Fiber Length. The direct shear tests were carried out on 9 groups of fiber-reinforced soil. The shear strength parameters of fiber-reinforced soil were calculated, and Table 4 lists the results of shear strength parameters (friction angle and cohesion).

From the test results in Table 4, the shear strength parameters of polypropylene fiber soil with different mixing ratios under F-T cycles were obviously different. Therefore, variance analysis and range analysis were conducted to examine the influences of three factors on mechanical properties of fiber soil in order to determine the optimum combination of fiber-reinforced soil under F-T cycles.

The basic principle of analysis of variance (ANOVA) is to calculate variance (MS) by squared sum (SS) and degree of freedom (DF) and then calculate F value. If $F > F\alpha$ (DF_f, DF_e), where DF_f is degree of freedom caused by factors and DF_e is degree of freedom caused by error, it indicates that the influencing factors are significant. In order to calculate the variance for the orthogonal experiment, the sum of squares of total deviations and total degree of freedom should be decomposed firstly, as listed below:

$$SS_T = SS_f + SS_e, \tag{1}$$

where SS_T is the sum of squares of total deviations; SS_f is the sum of squares of deviations caused by factors; and SS_e is the sum of squares of deviations caused by error.

$$DF_T = DF_f + DF_e, \tag{2}$$

where DF_T is the total degree of freedom.

Based on the sum of squares of deviations and degree of freedom, the variance of factor column and error column can be calculated by

$$MS_f = \frac{SS_f}{DF_f}, \qquad MS_e = \frac{SS_e}{DF_e}, \tag{3}$$

where MS_f is variances caused by factors and MS_e is variances caused by error.

According to the variance values, the F statistic can be constructed and analyzed:

Table 4: Shear strength parameters of fiber-reinforced soil specimens.

Group serial number	Internal friction angle (°)	Cohesion (kPa)
1	34.99	68.06
2	34.99	58.18
3	33.53	66.74
4	32.08	51.37
5	27.89	61.85
6	29.80	56.58
7	28.11	53.54
8	31.91	50.03
9	23.02	50.22

$$F_f = \frac{MS_f}{MS_e}. \tag{4}$$

ANOVA results are given in Table 5. The variance sources are namely F-T cycles, fiber length, fiber content, and empty column, respectively.

ANOVA results showed that the effect of each influencing factor on internal friction angle was not significant. However, F-T cycles presented a significant effect on the internal friction angle due to $F_{0.05}$ (2, 6) > 4.35 > $F_{0.10}$ (2, 6). The influences of fiber length and fiber content on internal friction angle were submerged by error. As a result of 21.24 > $F_{0.01}$ (2, 6), F-T cycles had a great influence on the cohesion of soil, which was the main significant influencing factor. According to $F_{0.01}$ (2, 6) > 7.87 > $F_{0.05}$ (2, 6), the influence of fiber content on the cohesion of soil is remarkable while the influence of fiber length on the cohesion of soil is not significant.

A range analysis of various factors was carried out, and the results are presented in Table 6. The mean K_j and the extreme value of the three factors at each test level were calculated, and the variation tendency of shear strength parameters with the influence factors is shown in Figures 3 and 4.

In the light of the range analysis results, the influencing order of main factors was I > III > II (13.064 > 7.959 > 3.437) for cohesion of fiber soil. F-T cycles had the greatest influence on cohesion index, followed by fiber content and fiber length. The cohesion decreases with the increase of F-T cycles, and the downward trend was slow. The trend of cohesion of fiber soil was consistent with that of general soil under F-T cycles. With the increase of fiber length, cohesion showed the trend of increasing first and then becoming smaller which had the maximum value when the fiber length is 9 mm. Since the fiber is an isotropic material in soil, when the fiber length is too short, the fiber-reinforcing effect is weakened based on principle of friction between reinforcement and soil [34], and the overall strength enhancement effect of the fiber soil is not obvious; when the fiber length is too long, although the fibers are meshed between the fibers, the effect of the isotropic distribution is reduced in the soil. Obviously, with the increase of fiber content, cohesive force of soil increases significantly.

For the internal friction angle of soil, the ordering of factors was consistent with previous ordering of cohesion, but its range value was smaller than that of cohesive force.

Table 5: Analysis of variance (ANOVA) results for mechanical index.

Assessment index	Source of variance	SS	DF	Error sources	F value	Critical value	Significance
Internal friction angle (°)	F-T cycles	72.57	2		4.35	$F_{0.01}$ (2, 6) = 10.90 $F_{0.05}$ (2, 6) = 5.14 $F_{0.10}$ (2, 6) = 3.46	*
	Fiber length	2.06	2	√			
	Fiber content	27.21	2	√			
	Empty column	50.02	2	√			
Cohesion (kPa)	F-T cycles	258.84	2		21.24	$F_{0.01}$ (2, 4) = 18.00 $F_{0.05}$ (2, 4) = 6.94 $F_{0.10}$ (2, 4) = 4.32	***
	Fiber length	20.95	2	√			
	Fiber content	95.94	2		7.87		**
	Empty column	24.37	2	√			

Note. √, the item of error sources; ***, most significant; **, more significant; *, significance.

Table 6: Analysis of variance (ANOVA) results for mechanical index.

Assessment index	Range	I F-T cycles	II Fiber length	III Fiber content	IV Empty column
Cohesion (kPa)	K_1	64.326	56.101	53.192	56.747
	K_2	56.600	59.538	57.845	57.216
	K_3	51.262	56.549	61.151	58.225
	R	13.064	3.437	7.959	1.478
Internal friction angle (°)	K_1	34.503	30.967	32.993	28.633
	K_2	29.923	31.110	28.783	31.240
	K_3	27.680	30.030	30.330	32.233
	R	6.823	1.080	4.210	3.600

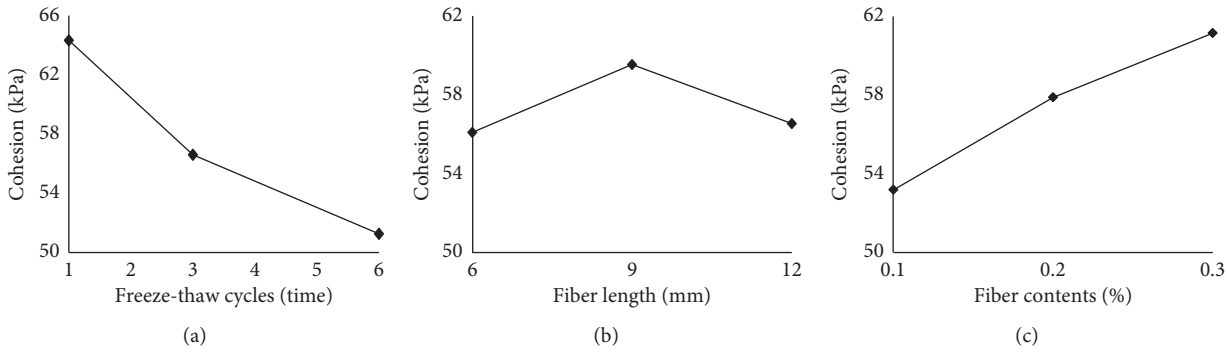

Figure 3: Tendency of the cohesion with influencing factors: (a) freeze-thaw cycles; (b) fiber length; (c) fiber contents.

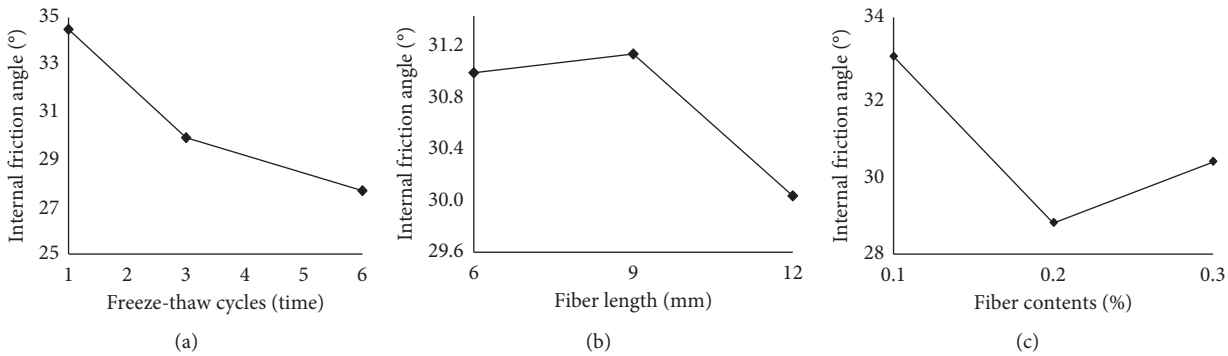

Figure 4: Tendency of the angle of internal friction with influencing factors: (a) freeze-thaw cycles; (b) fiber length; (c) fiber contents.

The effects of fiber and F-T cycles on internal friction angle were smaller than cohesion.

The optimum combination scheme should be determined on the basis of the orthogonal experiment results. The basic principle of determining the optimum level combination under various factors was to determine the main assessment indexes firstly, and then the best combination scheme was determined based on the principle that main indicators, significant indicators, and large fluctuations in the indicators were given priority. In the evaluation index of this test, cohesive force made a great deal of difference on the shear strength of soil, and the numerical fluctuation of each level was also obvious, which was the main influence index. Therefore, the optimum combination scheme was a combination scheme with a fiber length of 9 mm and the fiber content of 0.3%.

3.2. Comparative Analysis of Shear Strength Parameters between Fiber-Reinforced Soil and Ordinary Soil. Table 7 and Figure 5 presented the shear strength parameters of fiber-reinforced soil and ordinary soil under the optimum fiber content and fiber length.

As observed from Figure 5(a), the internal friction angle of plain soil increases gradually with the increase of F-T cycles, and the enhancement effect was the most remarkable between one F-T cycle and three F-T cycles. The internal friction angle of fiber soil in the first F-T cycle has been greatly enhanced. With the increasing of F-T cycles, the internal friction angle decreased. After three F-T cycles, the internal friction angle of fiber-reinforced soil was smaller than that of ordinary soil. Due to the presence of fibers, the water film is more likely to adhere to the surface of fiber. During the freezing process, the ice crystals along the fiber distribution made the structure more completely broken, the increase in the number of pores, the pore shape direction tend to be irregular, longitudinal cracks deep, and irregular shapes appear in the original complete place. Rearranging these will cause the soil particles to be in close contact with them and increases the point of contact between the soil particles which make the arrangement more rough. Therefore, it was conducive to play the friction between particles to increase friction and increase the internal friction angle, but the interwoven point between fibers increased after F-T, and the interweaving mechanism between fibers was more obvious which was conducive to the increase of cohesion; consequently, the internal friction angle will also decrease.

It is obvious from Figure 5(b) that the cohesion of ordinary soil and fiber-reinforced soil decreased gradually with the increase of F-T cycles, while the decrease tendency of cohesion decreased. At the first F-T cycle, the cohesion declined most significantly. The cohesion of the fiber-reinforced soil was greater than that of the ordinary soil under the same F-T cycles, and the cohesion of fiber-reinforced soil was stronger than that of clay with the increase of F-T cycles. With the increase of F-T cycles, the strengthening effect of fiber and soil on cohesive force of soil was increasing gradually. When the fiber was added, the fiber had a negative charge, which can collect the water film between the soil particles and the fiber. It can transfer the tension and strengthen the cohesive force of the whole soil mass.

4. Stability Analysis of Embankment Slope

4.1. Computational Model. The analysis process on stability of the fiber-reinforced soil slope was expounded by using the typical high-fill soil slope in northeast China which can be seen in Figure 6. The finite element model of the high-fill soil slope was established based on the finite element analysis software ANSYS, and considering that the size of the road in the length direction was much larger than that on its cross section, the road slope could be simplified as a plane problem. Because of the symmetry of road to its centerline, only half of the cross section of the finite element model was established, and symmetric constraint was applied to the symmetry line to improve the computational efficiency. The finite element model of road slope was established by using the plane element PLANE82 provided in Figure 7, which had 8 nodes, and each node had two degrees of freedom with high accuracy and adaptability to irregular grid strong.

The constitutive model of soil was a significant factor in the stability analysis of soil slope. The constitutive model of soil mainly includes D-P (Drucker-Prager) model, Cambridge model, and Duncan-Zhang model, among which the most commonly used is D-P model, so the D-P model was also chosen in this paper. In the D-P model, the equivalent stress σ_e can be obtained by equation (5) and Von Mises yield formula can be expressed as equations (6) and (7):

$$\sigma_e = 3\beta\sigma_m + \left[\frac{\{s\}^T[M]\{s\}}{2}\right]^{1/2}, \tag{5}$$

$$F = 3\beta\sigma_m + \left[\frac{\{s\}^T[M]\{s\}}{2}\right]^{1/2} - \sigma_y = 0, \tag{6}$$

$$\sigma_y = \frac{6C\cos\phi}{\sqrt{3}(3-\sin\phi)}, \tag{7}$$

where σ_m is the hydrostatic pressure, β is the material parameter determined by internal friction angle φ; $\{s\}$ is the deviation stress matrix; C is the cohesive force; and φ is the soil expansion angle. Therefore, when using the D-P model to set the material properties, two basic mechanical parameters of material need to be set: cohesive force C and internal friction angle φ. The finite element model using the measured shear strength parameters is listed in Table 7. The other material parameters are as follows: Es = 100 MPa, Poisson's ratio $\mu = 0.32$, and soil density based on the maximum dry density $\rho d\max = 1.87\ \mathrm{g/cm^3}$.

When using the finite element method to analyze slope stability, there are two key problems to be solved which are the judgment criteria of slope instability and the quantitative expression of slope stability. Zienkiewic put forward that the convergence of calculation model can be used to judge whether the slope is unstable or not when using finite

Table 7: Shear strength parameters of fiber-reinforced soil and ordinary soil under F-T cycles.

Soil type	Cycle times of F-T	Cohesion (kPa)	Internal friction angle (°)
Fiber-reinforced soil	0	96.82	19.18
	1	71.36	37.88
	3	61.85	27.89
	6	57.85	27.22
Ordinary soil	0	95.45	21.04
	1	63.50	21.74
	3	51.37	32.88
	6	45.09	33.88

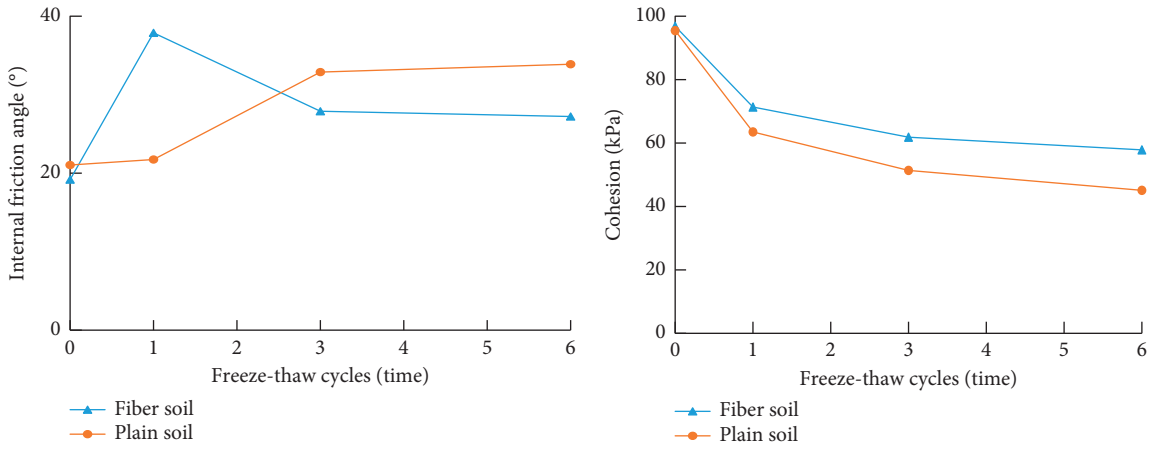

Figure 5: Shear strength index contrast of fiber soil and soil under the freezing and thawing: (a) internal friction angle; (b) cohesion.

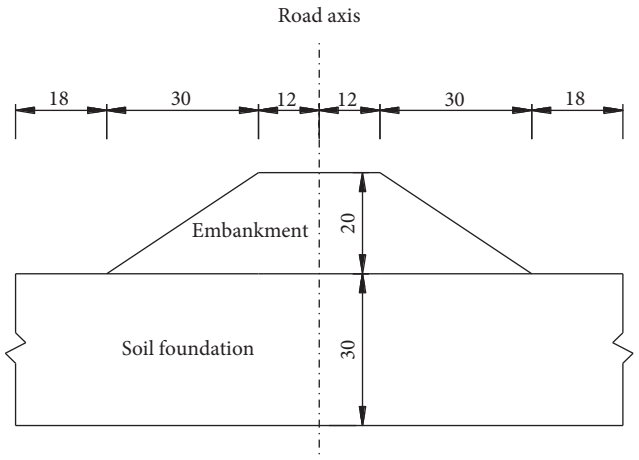

Figure 6: Size of embankment slope (unit: m).

element method to calculate slope stability [35]. It was proposed that the number of iterations is 1000 and the relative difference of node displacement is less than 0. 001 which can be both regarded as convergence criterion [36]. In this paper, the convergence of finite element model was used as the criterion of slope instability, which means that if the finite element model converges, the slope is stable; otherwise, the slope is considered unstable. The convergence criterion of Reference [36] was used to determine whether the finite element model converges in this study.

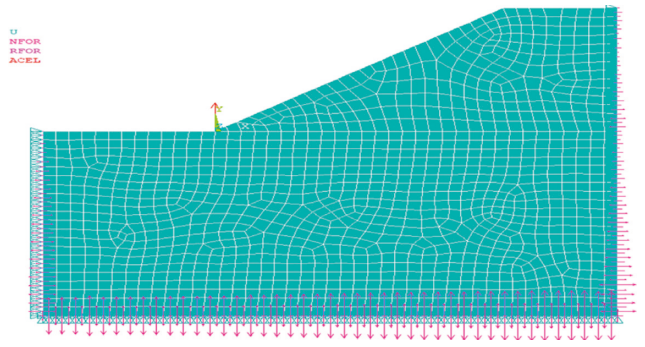

Figure 7: The finite element model of road slope.

The strength reduction method was selected to realize the quantitative expression of slope stability. The formulas for calculating the shear strength parameters Cohesion C' and the internal friction angle φ' after reduction are as follows:

$$C' = \frac{C}{F},$$
$$\tan \phi' = \frac{\tan \phi}{F}. \tag{8}$$

In accordance with the definition of strength reduction coefficient, the coefficient can objectively reflect the magnitude of slope stability, that is, it can realize the quantitative

expression of slope stability, which was called slope stability coefficient in this paper. The calculation process of the slope stability coefficient is as follows: (1) let F take a small value and calculate the reduced shear strength parameters C', φ' by equation (8); (2) the shear strength parameters were input into the finite element model, and the model was solved. If the model converges, the slope is considered to be stable; (3) increase the F value gradually (take a small increment, such as 0.01) and repeate the steps (1) and (2) until the finite element model does not converge; the obtained F value was the slope stability coefficient.

4.2. Stability Analysis. In the slope stability analysis, two kinds of loadings were applied to finite element model; one was the dead weight of soil slope which was applied to the whole slope, and the other was the uniformly distributed loading which was applied to the top of the finite element model for 98 kPa/m to simulate the vehicle load. Under the optimal fiber content and fiber length, the stability coefficients of fiber reinforced soil and ordinary slope under 0, 1, 3, and 6 F-T cycles were obtained. The maximum plastic strain and maximum horizontal displacement of the slope were calculated by using the proposed slope stability analysis method, respectively. The stability coefficient results are shown in Figure 8, the maximum plastic strain of the slope can be seen in Figures 9 and 10 presents the maximum horizontal displacement of the slope.

As observed in Figure 8, the slope stability coefficients of subgrade slope for each group showed that the stability coefficients of the ordinary soil slope and fiber-reinforced soil slope were the same before F-T cycle. Under the condition of one F-T cycle, the stability of the fiber-reinforced soil subgrade slope was improved, and the slope stability coefficient was increased by 42.86%, but the reinforcement effect of fiber soil was gradually weakened with the increase of F-T cycles. After three F-T cycles, the effect of fiber-reinforced soil on subgrade stability gradually stabilized.

It is obvious from Figure 9 that the plastic strain of both fiber-reinforced soil and ordinary soil is very small when the stability coefficient is less than a certain value. The plastic strain increases with the increase of stability coefficient, but the growth rate is slow. When the stability coefficient increases by a certain value (near the slope instability), the plastic strain increases rapidly and the plastic zone of subgrade slope will develop into a penetrating zone; the slope is in the unstable stage at this time. It can also be obtained from Figure 10 that when the stability coefficient of both fiber-reinforced soil and ordinary soil is less than a certain value, the horizontal displacement is very small. The horizontal displacement increases with the increase of stability coefficient, but the growth rate is slow. When the stability coefficient increases by a certain value (near the slope instability), the horizontal displacement increases rapidly, and the slope has the possibility of sliding at this moment. The calculation results of plastic strain in Figure 8 and horizontal displacements in Figure 10 are in good agreement with the calculated slope stability coefficient results, which is also a good verification of the slope stability analysis method. Moreover, a meaningful phenomenon can be found from

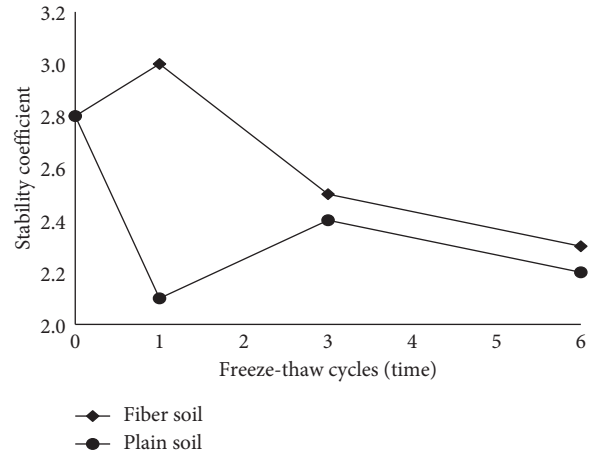

Figure 8: Slope stability coefficient.

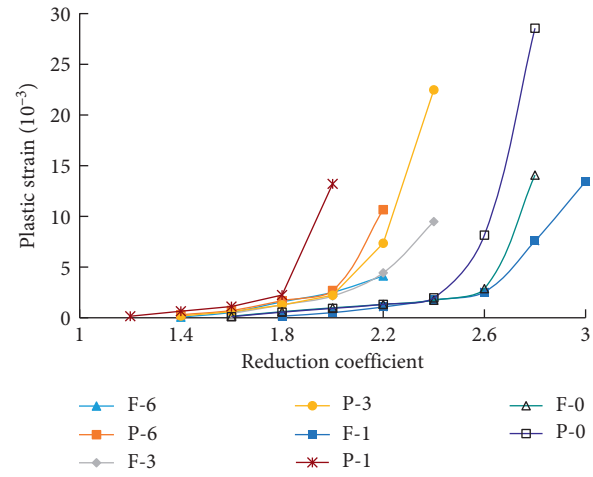

Figure 9: Plastic strain. P-0: plain soil of 0 F-T cycles; F-0: fiber soil of 0 F-T cycles; P-1: plain soil of 1 F-T cycle; F-1: fiber soil of 1 F-T cycle; P-3: plain soil of 3 F-T cycles; F-3: fiber soil of 3 F-T cycles; P-6: plain soil of 6 F-T cycles; F-6: fiber soil of 6 F-T cycles.

Figures 9 and 10 that the plastic strain and horizontal displacement change obviously when the slope is near instability but not yet unstable, which may provide ideas for monitoring and early warning of fiber-reinforced soil slopes and ordinary soil slopes.

5. Conclusions

In this study, polypropylene fiber was used to strengthen a common clay in northeast China, and the optimum fiber content and fiber length were determined by direct shear test considering the effect of F-T cycle. Then, the shear strength parameters of fiber-reinforced soil with the optimum fiber content and fiber length were tested. The stability analysis method of soil slope was put forward, and the stability of typical high-fill soil slope in northeast China was calculated based on the finite element method and strength reduction method. On the basis of the research work of this paper, the following conclusions could be drawn:

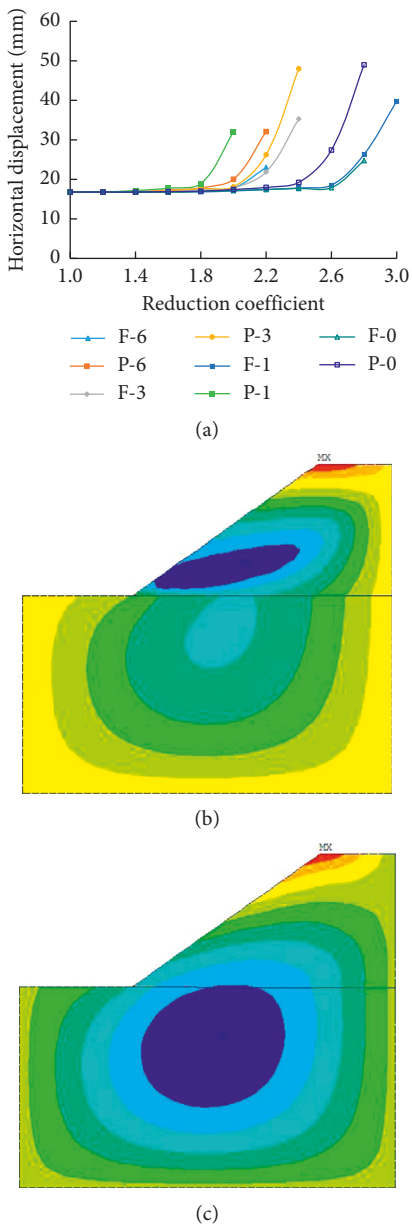

Figure 10: Horizontal displacement: (a) displacement calculation result; (b) cloud picture of displacement of ordinary soil under the action of 1 time F-T cycle at $F = 2.0$; (c) cloud picture of displacement of fiber-reinforced soil under the action of 1 time F-T cycle at $F = 2.0$.

(i) With the increase of F-T cycles, the cohesion difference between polypropylene fiber and soil increased gradually, and the reinforcement effect of internal friction angle was remarkable under one F-T cycle.

(ii) According to direct shear test, the optimum combination scheme can be obtained. The fiber-reinforced soil has the best enhancement effect when the fiber content is 0.3% and the fiber length is 9 mm.

(iii) The stability analysis method of soil slope combining finite element method and strength reduction method could be used to analyze the stability of polypropylene fiber-reinforced soil slope and ordinary soil slope, results of which were accurate and reliable.

(iv) The slope stability of fiber-reinforced soil embankment slope was better than that of ordinary soil embankment slope. With the increase of F-T cycles, the stability of polypropylene fiber-reinforced soil embankment slope with the optimal combination scheme was weakened, but the stability of fiber soil slope was significantly improved under one F-T cycle.

(v) It should be pointed that the plastic strain and horizontal displacement had obvious changes when the slope was near instability but not yet unstable, which may provide some ideas for the monitoring and early warning of fiber-reinforced soil slope and ordinary soil slope.

Data Availability

The data used to support the findings of this study are included within the article. The data are available from the corresponding author upon request.

Conflicts of Interest

The authors declare that there are no conflicts of interest regarding the publication of this paper.

Acknowledgments

This work was supported by the National Natural Science Fund of China (Grant no. 51408258), Transportation Technology Program of Jilin Province of China (Grant nos. 2018ZDGC-16, 2013-1-8, and 2018-1-9), Training Program for Outstanding Young Teachers of Jilin University, and Science and Technology Project of the 13th Five-Year Plan of Department of Education Jilin Province of China (Grant nos. JJKH20190015KJ and JJKH20190150KJ). We would like to acknowledge the following people from Northeast Forestry University for technical support in testing procedure and data processing: Sun Hao, Wang Zhongzhi, and Fang Liqun.

References

[1] W. He, W. Gao, G. F. Wang, and D. L. Zhao, "Cause and control of soil-cutting's sliding collapse in frigid zone," *Journal of Natural Disasters*, vol. 15, no. 3, pp. 66–70, 2006.

[2] P. J. Cleall, H. R. Thomas, M. C. Glendinning et al., "Modelling the behaviour of freezing and thawing soil slopes," in *Proceedings of International Congress on Environmental Geotechnics*, pp. 1603–1610, Wales, UK, June 2006.

[3] K. J. Tsai, H. Y. Wang, S. C. Chen, and Y. M. Sung, "Effect of soil freezing and thawing behavior on slope stability," *International Society of Offshore and Polar Engineers*, vol. 1, pp. 800–810, 1999.

[4] Y. Guo and W. Shan, "Monitoring and experiment on the effect of freeze-thaw on soil cutting slope stability," *Procedia Environmental Sciences*, vol. 10, no. 1, pp. 1115–1121, 2011.

[5] Y. Guo, W. Shan, H. Jiang, Y. Y. Sun, and C. C. Zhang, "The impact of freeze–thaw on soil cut slope stability and reinforcement of shrub roots in high-latitude frozen regions," *Environmental and Engineering Geology*, no. 202999, pp. 19–22, 2014.

[6] S. S. Subramanian, T. Ishikawa, S. Yokohama, and T. Tokoro, "Numerical simulation of volcanic soil slope failure under coupled freeze-thaw and rainfall infiltration effects," *Japanese Geotechnical Society Special Publication*, vol. 1, no. 7, pp. 5–10, 2015.

[7] H. Wu, Q. Ge, and J. B. Tian, "Study on the shear strength parameters under different freezing and thawing cycles of soil slope in China," *Applied Mechanics and Materials*, vol. 454, pp. 222–225, 2014.

[8] D. Chang, J. K. Liu, L. Xu, and Q. M. Yu, "Experiment study of effects of freezing-thawing cycles on mechanical properties of Qinghat-Tibet silty sand," *Chinese Journal of Rock Mechanics and Engineering*, vol. 33, no. 7, pp. 1496–1502, 2014.

[9] H. H. Cui, J. K. Liu, L. Q. Zhang, and Y. H. Tian, "A constitutive model of subgrade in a seasonally frozen area with considering freeze-thaw cycles," *Rock and Soil Mechanics*, vol. 36, no. 8, pp. 2228–2236, 2015.

[10] A. J. Klemm and P. Klemm, "The effects of the alternate freezing and thawing cycles on the pore structure of cementitious composites modified by MHEC and PVA," *Building and Environment*, vol. 32, no. 6, pp. 509–512, 1997.

[11] A. Aldaood, M. Bouasker, and M. Al-Mukhtar, "Effect of water during freeze-thaw cycles on the performance and durability of lime-treated gypseous soil," *Cold Regions Science and Technology*, vol. 123, pp. 155–163, 2016.

[12] A. Aldaood, M. Bouasker, and M. Al-Mukhtar, "Impact of freeze-thaw cycles on mechanical behaviour of lime stabilized gypseous soils," *Cold Regions Science and Technology*, vol. 99, pp. 38–45, 2014.

[13] C. Han and P. Cheng, "Micropore variation and particle fractal representation of lime-stabilised subgrade soil under freeze-thaw cycles," *Road Materials and Pavement Design*, vol. 16, no. 1, pp. 19–30, 2014.

[14] R. L. Parsons and J. P. Milburn, "Engineering behavior of stabilized soils," *Transportation Research Record: Journal of the Transportation Research Board*, vol. 1837, pp. 20–29, 2018.

[15] S. Arora and A. H. Aydilek, "Class F fly-ash-amended soils as Highway base materials," *Journal of Materials in Civil Engineering*, vol. 17, no. 6, pp. 640–649, 2015.

[16] J. T. Laba and J. B. Kennedy, "Reinforced earth retaining wall analysis and design," *Canadian Geotechnical Journal*, vol. 23, no. 3, pp. 317–326, 1986.

[17] M. N. Ensan and I. Shahrour, "A simplified elastoplastic macroscopic model for the reinforced earth material," *Mechanics Research Communications*, vol. 27, no. 1, pp. 79–86, 2000.

[18] P. D. Buhan, R. Mangiavacchi, R. Nova, G. Pellegrini, and J. Salençon, "Yield design of reinforced earth walls by a homogenization method," *Geotechnique*, vol. 39, no. 2, pp. 189–201, 1989.

[19] A. R. Estabragh, A. T. Bordbar, and A. A. Javadi, "A study on the mechanical behavior of a fiber-clay composite with natural fiber," *Geotechnical and Geological Engineering*, vol. 31, no. 2, pp. 501–510, 2012.

[20] A. E. M. K. Mohamed, "Improvement of swelling clay properties using hay fibers," *Construction and Building Materials*, vol. 38, pp. 242–247, 2013.

[21] Y. K. Wu, Y. B. Li, and B. Niu, "Investigation of mechanical properties of randomly distributed sisal fibre reinforced soil," *Material Research Innovations*, vol. 18, pp. 953–959, 2015.

[22] T. Maliakal and S. Thiyyakkandi, "Influence of randomly distributed coir fibers on shear strength of clay," *Geotechnical and Geological Engineering*, vol. 31, no. 2, pp. 425–433, 2012.

[23] S. Akbulut, S. Arasan, and E. Kalkan, "Modification of clayey soils using scrap tire rubber and synthetic fibers," *Applied Clay Science*, vol. 38, no. 1, pp. 23–32, 2007.

[24] A. S. Zaimoglu, Y. Calik, R. K. Akbulut, and T. Yetimoglu, "A study on freeze-thaw behavior of randomly distributed fiber-reinforced soil," *Periodica Polytechnica Civil Engineering*, vol. 60, no. 1, pp. 3–9, 2016.

[25] M. Roustaei, A. Eslami, and M. Ghazavi, "Effects of freeze-thaw cycles on a fiber reinforced fine grained soil in relation to geotechnical parameters," *Cold Regions Science and Technology*, vol. 120, pp. 127–137, 2015.

[26] M. Ghazavi and M. Roustaie, "The influence of freeze-thaw cycles on the unconfined compressive strength of fiber-reinforced clay," *Cold Regions Science and Technology*, vol. 61, pp. 125–131, 2010.

[27] K. Hazirbaba and H. Gullu, "California bearing ratio improvement and freeze-thaw performance of fine-grained soils treated with geofiber and synthetic fluid," *Cold Regions Science and Technology*, vol. 63, pp. 50–60, 2010.

[28] Ministry of Transport of the People's Republic of China, *Test Methods of Soils for Highway Engineering*, Ministry of Transport of the People's Republic of China, Beijing, China, 2007.

[29] B. Hui and H. E. Ping, "Influence of freeze-thaw cycles on physical and mechanical properties of salty soil," *Chinese Journal of Geotechnical Engineering*, vol. 12, pp. 1958–1962, 2009.

[30] X. T. Hu, B. Liang, Y. J. Chen, Q. Xue, and Y. Wan, "Mechanical and microstructural properties changes of solidified sewage sludge due to cyclic freezing and thawing," *Rock and Soil Mechanics*, vol. 37, no. 5, pp. 1317–1323, 2016.

[31] L. Yang, J. Zhu, and H. Jiao, "Performance research on the calcareous soil foundation with TG curing agent under freeze and thaw cycles," *Journal of Glaciology and Geocryology*, vol. 37, no. 4, pp. 1016–1022, 2015.

[32] A. L. Welker and N. Josten, "Interface friction of a geomembrane with a fiber reinforced soil," in *Proceedings of GeoFrontiers Congress 2005*, pp. 1–8, Austin, TX, USA, October 2005.

[33] Ministry of Transport of the People's Republic of China, *Technical Specifications for Construction of Highway Subgrade*, Ministry of Transport of the People's Republic of China, Beijing, China, 2006.

[34] C.-S. Tang, X.-J. Pei, D.-Y. Wang, B. Shi, and J. Li, "Tensile strength of compacted clayey soil," *Journal of Geotechnical and Geoenvironmental Engineering*, vol. 141, no. 4, pp. 04014122–04014130, 2015.

[35] O. C. Zienkiewicz and R. L. Taylor, *The Finite Element Method*, McGraw-Hill, New York, NY, USA, 4th edition, 1989.

[36] D. V. Griffiths and P. A. Lane, "Slope stability analysis by finite elements," *Géotechnique*, vol. 49, no. 3, pp. 387–403, 1999.